



13th World Conference on Earthquake Engineering
Vancouver, B.C., Canada
August 1-6, 2004
Paper No. 949

CONTROLLING SEISMIC RESPONSE WITH SHAPE MEMORY ALLOY DEVICES

Michael J. WESOLOWSKY¹ and John C. WILSON²

SUMMARY

Recently, interest has emerged in investigating the potential for use of advanced materials in developing new and innovative structural response modification devices for seismic applications, such as for seismic isolator and damping systems. Shape memory alloys (SMAs) are a class of metals that have the capability to dissipate energy through repeated cycling loading without significant permanent deformations. They have a high usable strain range (up to about 8%) compared to other metals, and thus require a smaller volume of material in order to produce the same damping capacity. They also possess an inherent ability to provide stiff elastic resistance at large displacements. One of the most promising of these alloys is a material composed of essentially equal percentages of nickel and titanium (Nitinol). Although relatively commonplace in other fields such as biomedical applications, the development of SMA devices for seismic applications is still in the infancy stages. Consequently, fundamental studies of their basic behavioural characteristics are crucial. In this paper we report our study that examines the response of a wide range of single-degree-of-freedom systems modified with various SMA devices. These fundamental systems have been subjected to near-field and far-field earthquakes ground motions scaled to two levels of peak ground velocity (because of the nonlinear nature of the SMA response). Hysteretic responses have been evaluated to compare the behaviours over a range of SMA device characteristics. Results show that a clearly defined period exists above which the strains within the SDOF system become unacceptably large. For these systems the SMA device must be reconfigured to ensure strain behaviour is within acceptable limits. This period varies with earthquake scaling, device type and supplemental damping. Further, a balance must be struck between the natural period of the system and the hysteretic characteristics of the damper in order to produce responses that meet the goals of seismic isolation, which include reduced forces and accelerations at the expense of increased displacements.

¹ Ph.D. Candidate, Department of Civil Engineering, McMaster University, Hamilton, ON, Canada. E-mail: wesolomj@mcmaster.ca

² Associate Professor, Department of Civil Engineering, McMaster University, Hamilton, ON, Canada. E-mail: jcwilson@mcmaster.ca

INTRODUCTION

Shape Memory Alloys (SMAs) (Funakubo [1]) are a class of alloys that have the capability to dissipate energy through repeated cycling loading without significant permanent deformations. They have an unusually high usable strain range compared to other metals, and thus require a smaller volume of material in order to produce the same damping capacity. The most common SMA used for seismic application is NiTi (commonly referred to as Nitinol), which is composed of approximately equal proportions of nickel and titanium. Other types of SMAs are available, often composed of copper and zinc, as well as many others. The study and use of SMAs is rapidly expanding, with many diverse applications such as medical, ballistics and aerospace engineering.

The behaviour of SMAs is dependent on the manufacturing process and the temperature range of alloying (annealing), which is the process of cooling the alloy. High alloying temperatures produce a fully austenite microstructure (a stable microstructural arrangement that typically has a body-centred cubic crystalline structure), which produces essentially linear elastic behaviour, while low alloying temperatures produce a fully martensite microstructure (a microstructural constituent produced by a diffusionless phase transformation) that produces behaviour which basically mimics standard bi-linear visco-plastic behaviour (with strain hardening). If an intermediate alloying temperature is applied, the behaviour contains elements of both austenitic and martensitic behaviour, and is known as a superelastic effect (Figure 1). In this scenario, the material loads in an elastic (austenite) manner, followed by a ‘plastic’ transformation phase, during which the microstructure transforms to become fully martensitic. At this point, the material becomes stiff, providing resistance for extreme loads. Upon unloading, the material follows the martensitic path until the transformation phase, which occurs at a lower ‘yield’ point than during loading. The material remains in the transformation phase until it reaches the original austenite path and returns to its starting point with little or no residual strain.

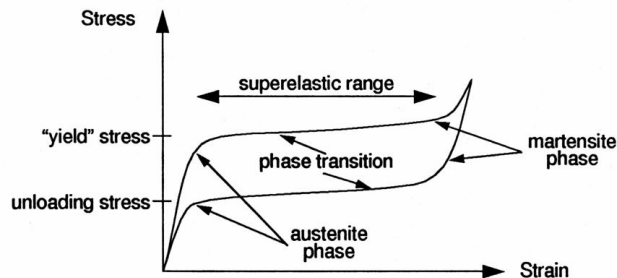


Figure 1. General form of Shape Memory Alloy superelastic behaviour. (Clark [2])

The behaviour is also dependant on the temperature of operation. Each SMA has a specific temperature known as the austenite finish temperature (A_f). Only when the material is strained at a temperature above A_f can the superelastic effect be realized. This temperature can range from -50°C to 110°C for Nitinol. If the material is strained below this temperature, there is no thermodynamic driving force to restore the austenite phase, and the material behaviour is analogous to SMAs created using low alloying temperatures (i.e. martensite). Further, each material has a temperature (known as M_d) above which an increase in stress will lead to permanent deformations of the austenite instead of a transformation to martensite, and thus the proper superelastic effect will not be realized. It is essential that the operating temperature of the SMA be kept between A_f and M_d in order for the optimal behaviour to occur. Dolce [3] provides a detailed description of the behaviour of NiTi in a simulated seismic test environment.

This paper outlines an extension of a widely-used model for the hysteretic behaviour of SMAs. Using this model, a parametric study has been conducted on the effects of introducing SMA-based structural modification devices to several single-degree-of-freedom systems (SDOFs). A traditional lead-rubber isolation system has also been evaluated for comparison. These fundamental systems have been subjected to near-field and far-field earthquakes ground motions scaled to two levels of peak ground velocity. Hysteretic responses have been evaluated to compare the behaviours over a range of SMA device characteristics.

EARTHQUAKE RECORDS

It is well-established that the qualitative effects of near-field motions are quite different from those of far-field records (Chopra [4]). The fault-normal acceleration component of near-field records usually contains a long-period pulse that is also visible in the velocity and displacement records. The consequences of these characteristics can be seen most notably by the large velocity and displacements incurred by structures located at near-fault locations (Kelly [5]). This can prove problematic for structures that are seismically isolated, as often large displacements can lead to instability in conventional isolators. It is frequently the practice to include supplemental dampers to control these large displacements, while accepting the negative side-effect of larger accelerations that are possible with heavy damping.

As a result of these consequences, it was decided to select two sets of records for this study, one set representing near-field ground motions, and one representing far-field ground motions. Near-field records were selected having a distance to the fault rupture of 8 km or less. Far-field records were selected having a distance to the fault rupture of 20 km or greater. Chopra [4] comments that near-field records have a ratio of peak ground velocity to peak ground acceleration that is remarkably higher than those for far-field records. This criterion was also used in the selection of the records. Table 1 gives details of the earthquake records selected. The near fault records are all fault-normal components.

Table 1. Earthquake records

Designation	Event	Station	Magnitude (M)	Distance to fault rupture (km)	pga (%g)	pgv (cm/s)	pgv/pga (sec)
NF1	Kobe, Japan (1995)	KJMA	6.9	0.6	0.85	95.7	0.11
NF2	Kobe, Japan (1995)	Takatori	6.9	0.3	0.68	169.5	0.25
NF3	Northridge (1994)	Rinaldi	6.7	7.1	0.89	173.1	0.20
NF4	Northridge (1994)	Sylmar74	6.7	6.2	0.59	130.3	0.22
NF5	Loma Prieta (1989)	Corralitos	6.9	5.1	0.48	45.5	0.10
NF6	Loma Prieta (1989)	LGPC	6.9	6.1	0.65	102.3	0.16
NF7	Kocaeli, Turkey (1999)	Yarimca	7.4	2.6	0.28	48.2	0.18
NF8	Kocaeli, Turkey (1999)	Izmit	7.4	4.8	0.15	22.6	0.15
NF9	Chi-Chi, Taiwan (1999)	CHY080	7.6	7	1.03	113.2	0.11
NF10	Chi-Chi, Taiwan (1999)	TCU084	7.6	0.01	1.15	112.7	0.10
FF1	Friuli, Italy (1976)	Tolmezzo	6.5	37.7	0.35	22.0	0.06
FF2	Friuli, Italy (1976)	Tolmezzo	6.5	37.7	0.32	30.8	0.10
FF3	Northridge (1994)	Stone Canyon	6.7	22.2	0.25	28.0	0.11
FF4	Northridge (1994)	Stone Canyon	6.7	22.2	0.39	38.0	0.10
FF5	Chi-Chi, Taiwan (1999)	TCU045	7.6	24.06	0.51	39.0	0.08
FF6	Chi-Chi, Taiwan (1999)	TCU045	7.6	24.06	0.47	36.7	0.08
FF7	Coalinga (1983)	Cantua Creek School	6.4	25.5	0.23	23.6	0.11
FF8	Coalinga (1983)	Cantua Creek School	6.4	25.5	0.28	25.8	0.09
FF9	Northridge (1994)	LA-Saturn St	6.7	30	0.47	34.6	0.07
FF10	Northridge (1994)	LA-Saturn St	6.7	30	0.44	39.0	0.09

HYSTERETIC MATERIAL MODEL

A widely-used model of SMA behaviour for seismic applications is that of Graesser [6]. This model captures the superelastic behaviour but does not include the martensitic hardening characteristics of SMAs, which are critical for 'fail-safe' action for extreme loads. The Wilde [7] model, an extension of the Graesser model, includes this behavioural characteristic and defines the relationship between a given change in strain and the resulting change in stress as:

$$d\sigma = E \cdot \left[d\varepsilon - |d\varepsilon| \cdot \left(\frac{\sigma - \beta}{Y} \right)^n \right] \cdot u_I(\varepsilon) + E_m \cdot d\varepsilon \cdot u_{II}(\varepsilon) + (3 \cdot a_1 \cdot d\varepsilon \cdot \varepsilon^2 + 2 \cdot a_2 \cdot \text{sign}(\varepsilon) \cdot d\varepsilon \cdot \varepsilon + a_3 \cdot d\varepsilon) \cdot u_{III}(\varepsilon) \quad (1)$$

where $d\sigma$ is the change in stress, E is the elastic modulus of the austenite phase (at small strains), $d\varepsilon$ is the applied change in strain, σ is the current stress, Y is the 'yield' stress at which the austenite-to-martensite transformation begins, and n is a constant controlling the sharpness of transition between elastic and superelastic states (see Figure 1). β is the one-dimensional back stress

$$\beta = E\alpha \left[\varepsilon_{in} + f_t |\varepsilon|^c \text{erf}(a\varepsilon)[u(-\varepsilon \cdot d\varepsilon)] \right] \quad (2)$$

where f_t , a and c are material constants controlling the type and size of the hysteresis, the amount of elastic recovery during unloading, and the slope of the unloading stress plateau, respectively. When $f_t = 0$ the model is purely martensitic; $f_t > 0$ gives superelastic behaviour. α is a constant that controls the slope of the stress-strain curve

$$\alpha = \frac{E_y}{E - E_y} \quad (3)$$

where E_y is the slope of the stress strain curve after 'yielding'. When $\alpha = 0$ the model is essentially elasto-plastic. ε_{in} is the inelastic strain:

$$\varepsilon_{in} = \varepsilon - \frac{\sigma}{E} \quad (4)$$

The error function

$$\text{erf}(x) = \frac{2}{\sqrt{\pi}} \cdot \int_0^x e^{-t^2} dt \quad (5)$$

is a convenient expression to model the return of the stress-strain curve during unloading so that with proper choice of f_t , a and c the inelastic stress is fully recovered at $\varepsilon = 0$. The unit step function

$$u(x) = \begin{cases} 1 & x \geq 0 \\ 0 & x < 0 \end{cases} \quad (6)$$

will activate the last term in Equation (2) only during unloading. Finally, the martensitic hardening is taken into account by:

$$u_I(\varepsilon) = (1 - u_{II}(\varepsilon) - u_{III}(\varepsilon)) \quad (8)$$

$$u_{II}(\varepsilon) = \begin{cases} 1 & |\varepsilon| \geq \varepsilon_m \\ 0 & \text{otherwise} \end{cases} \quad (9)$$

$$u_{III}(\varepsilon) = \begin{cases} 1 & \varepsilon \cdot d\varepsilon > 0 \quad \text{and} \quad \varepsilon_1 < |\varepsilon| < \varepsilon_m \\ 0 & \text{otherwise} \end{cases} \quad (10)$$

and where ε_1 is the strain at the beginning of the martensite transformation and ε_m is the strain when the transformation is complete. The second term involving E_m models the elastic behaviour of martensite and is non-zero only when $\varepsilon > \varepsilon_m$. The third term controls the transition from slope E_y to E_m and is non-zero

only when the total strain ϵ is within the (ϵ_1, ϵ_m) transition region during loading. The constants a_1, a_2, a_3 control the smoothness of the transition. Although the behaviour of the model is highly sensitive to the choice of numerical values for these three constants, once the values are set the model behaves quite well.

PARAMETRIC STUDY

The incremental formulation method for non-linear analysis (Clough [8]) was used in order to adapt the Wilde [7] model to be able to simulate the hysteretic behaviour of a SDOF system modeled with a SMA element subjected to earthquake accelerations. This study examines three hysteretic schemes: (1) traditional lead-rubber type bearings with no martensitic hardening (HS1), thick-looped SMA devices (HS2), and thin-looped SMA devices (HS3), and subjects SDOF systems to the near-field and far-field earthquakes. For each hysteretic scheme, four cases are considered (Table 2) which vary the superelastic plateau stress (Y) and the strain associated with martensitic hardening (ϵ_m). As an example, a comparison of each hysteretic scheme for case 4 can be found in Figure 2. For each case one linear-elastic response was computed using the stiffness of the austenitic phase of the SMA. This elastic scheme is referred to as ‘non-modified’. Each scheme with a non-linear element (HS1, HS2 and HS3) is referred to as ‘modified’. For comparisons, the ‘modified’ responses were normalized with respect to the ‘non-modified’ responses.

Table 2. Values of superelastic plateau stress (Y), strain at onset of martensite hardening (ϵ_1), and strain at fully martensitic behaviour (ϵ_m) for each case.

	Y (MPa)	ϵ_m
Case 1	200	0.06
Case 2	200	0.08
Case 3	500	0.06
Case 4	500	0.08

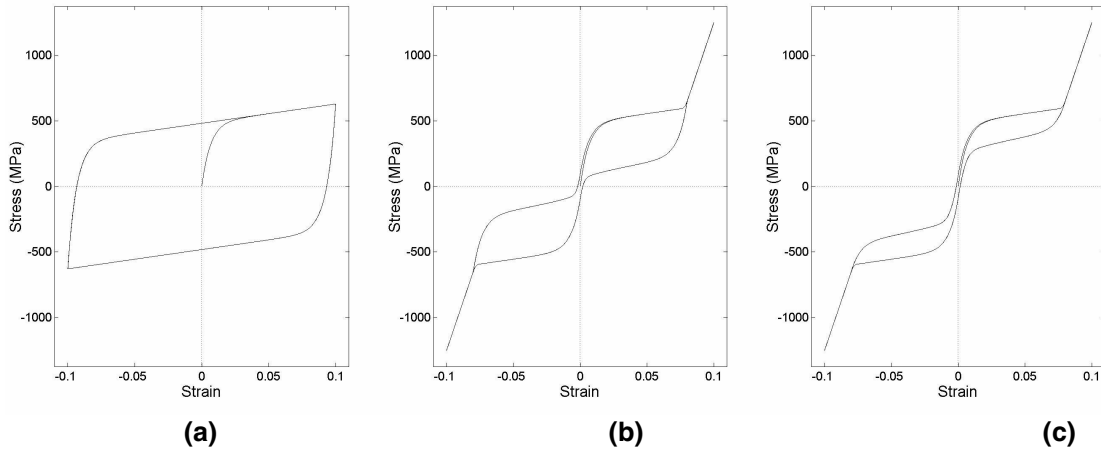


Figure 2. Hysteretic behaviour for case 4: (a) HS1, (b) HS2, and (c) HS3

Responses of Select Individual Single-Degree-of-Freedom Systems

Figure 3 shows the response for the SDOF system (case 4) having an elastic period of 0.5 seconds, subjected to earthquake NF1 (see Table 1) scaled to a peak ground velocity (pgv) of 20 cm/s. Modal damping of 5% has been added in parallel with the SMA element to model the inherent damping typical in many structural systems. This figure depicts the hysteretic behaviour for all three schemes (HS1-HS3). The elastic response of the non-modified SDOF system has been included for reference. The modified

schemes all produce strains that are larger than their non-modified counterpart, but the maximum stress in the hysteretic element has been reduced by a factor of almost three for all hysteretic schemes. HS1 is more effective than HS2 and HS3 in controlling displacements, however, the major drawback to HS1 is the residual strain (almost 0.02) that is clear in Figure 3b. Parametric studies on these systems have shown that the amount of residual strain is variable, and is dependent upon the earthquake ground motion. The system responses of HS2 and HS3 are similar, with comparable stresses and only slightly larger strains in HS3.

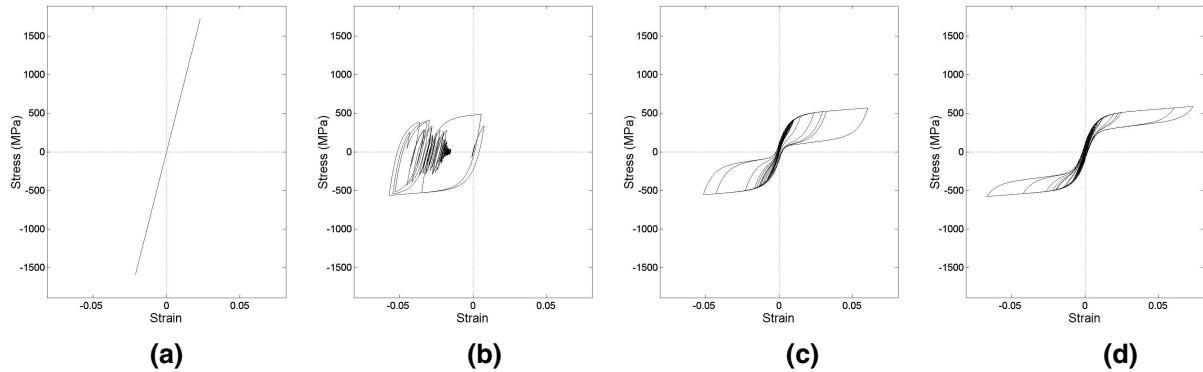


Figure 3. System response for NF1 (scaled to pgv = 20 cm/s, 5% damping) for (a) non-modified scheme, (b) HS1, (b) HS2, and (c) HS3

Figure 4 shows the response of the same system as in Figure 3 with a pgv of 40 cm/s. In this case, it is clear that the system strain is considerably larger than the results seen in Figure 3. Once again, HS1 provides better strain control than HS2 and HS3, with in this case only a small residual strain. Further, the system SMA strains for HS2 and HS3 have increased to 100% greater than the strain at the onset of martensitic hardening. This approaches the level of plastic deformation (which is not accounted for in the material model). The hysteretic behaviour also shows that HS2 and HS3 have stresses that approach those of the non-modified case and there is really no improvement in the stress response of the SMA- modified system. This highlights the delicate nature of the non-linear response of the system with regards to the level of system input.

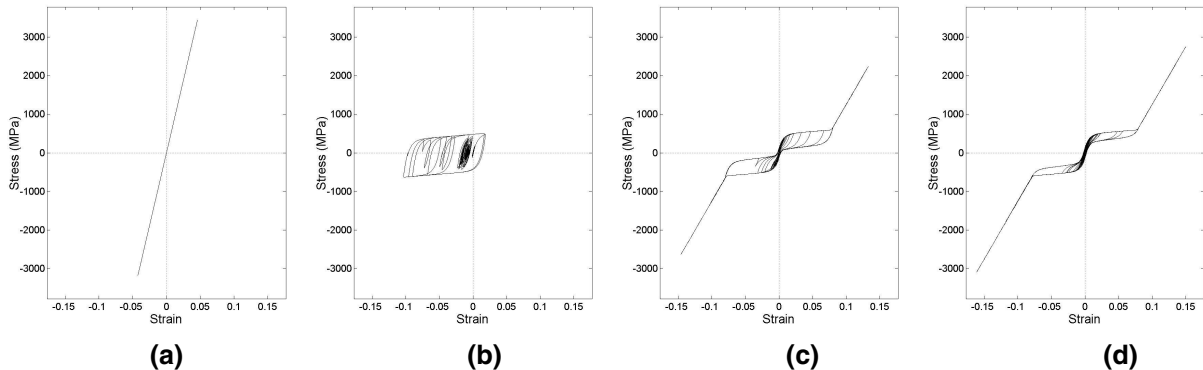


Figure 4. System response for NF1 (scaled to pgv = 40 cm/s, 5% damping) for (a) non-modified scheme (0.5 second period), (b) HS1, (b) HS2, and (c) HS3

Figure 5 shows the response of the system shown in Figure 4, but with a system damping of 25% (5% modal damping in parallel with 20% supplemental damping). The modified system strain has been considerably reduced relative to the 5% damped case shown in Figure 4; the system strain now barely reaches into the martensitic range for HS3, while HS2 remains in the superelastic range. HS1 is less affected by the effects of increased damping. Increased damping has also caused the maximum stress in the SMA element to be reduced by a factor of almost 7 compared to the non-modified case for all schemes.

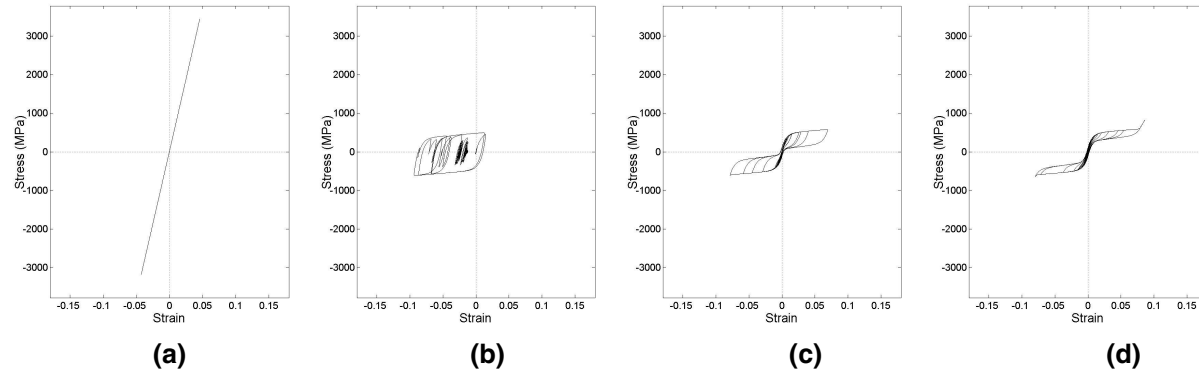


Figure 5. System response for NF1 (scaled to $\text{pgv} = 20 \text{ cm/s}$, 25% damping) for (a) non-modified scheme (0.5 second period), (b) HS1, (b) HS2, and (c) HS3

Mean Responses of Single-Degree-of-Freedom-Systems

The previous section (Figures 3-5) has presented responses for a single 0.5 second system. In this section variations of the SDOF mass have been considered, to produce a number of systems with a range of non-modified periods between 0 and 2 seconds. The non-modified case having an elastic stiffness equal to the austenite stiffness of the SMA system has also been considered for each period in order to compare modified to non-modified responses.

Figure 6 shows the mean maximum strain responses of the SDOF system to the near-field earthquakes as a function of period. The normalized maximum strains shown in the graphs have been determined by taking a ratio of modified strains to the non-modified case for that period. Thus, a value of 1 represents identical maximum mean strains for both modified and non-modified systems. Figure 6 presents the results for all three hysteretic schemes (HS1, HS2 and HS3), for both scalings of pgv (20 cm/s and 40 cm/s), for all four cases defined in Table 2, and for both 5% and 25% damping.

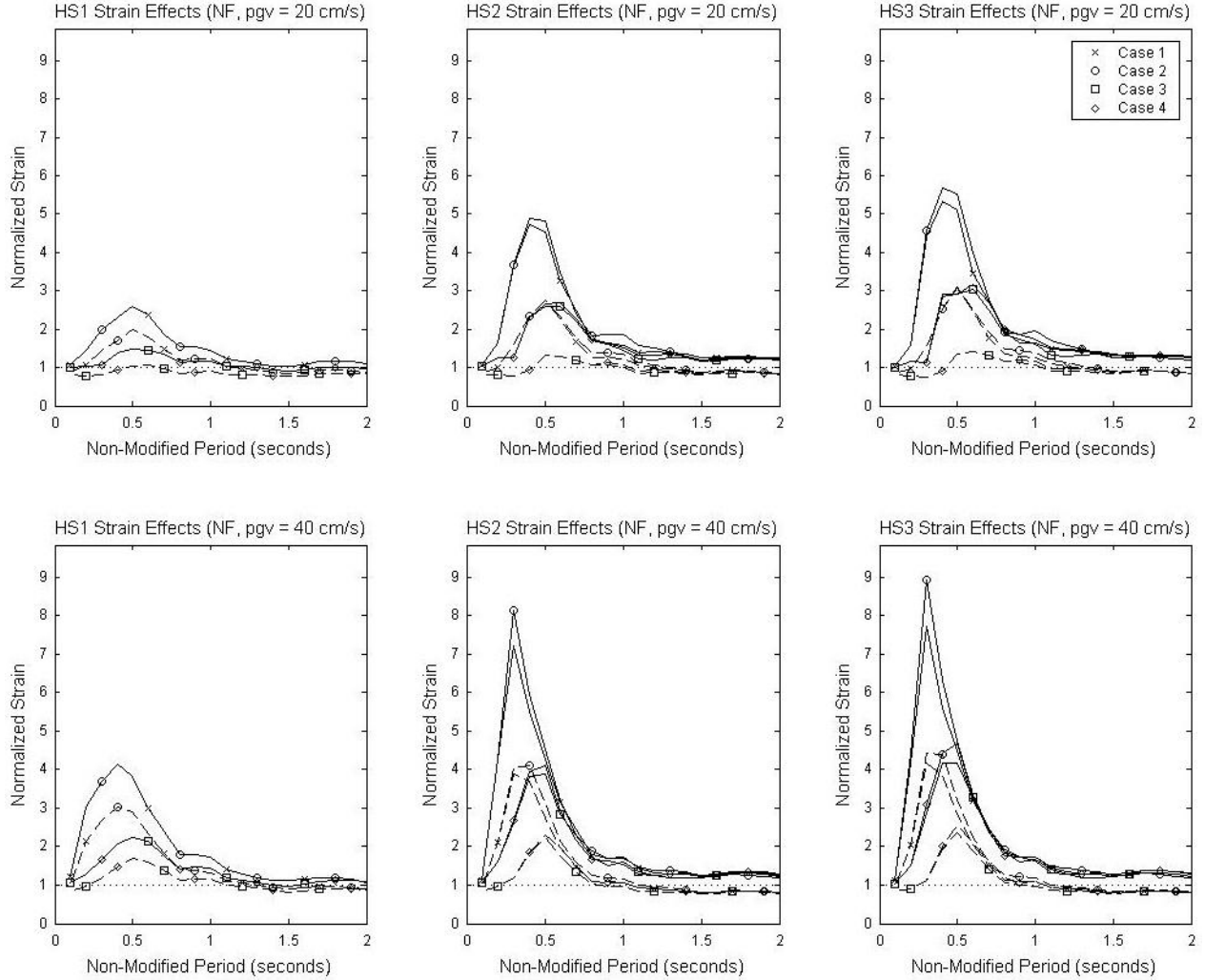


Figure 6. Maximum strain response for near-field earthquakes (solid line – 5% damping, dashed line – 25% damping)

For both pgv scalings, the strains provided by HS1 are the lowest for all non-modified periods. Since there is no martensitic hardening associated with HS1, both cases 1 and 2 have identical results, as do cases 3 and 4 (thus there are only four lines on the HS1 plots). For both HS2 and HS3, the cases with a ϵ_m of 8% had slightly larger strains than for those with 6%. This is due the increased overall stiffness of the system associated with a ϵ_m value of 6%. However, for HS2 and HS3, the differences between cases 1 and 2, and 3 and 4, are relatively minor. This leads to the conclusion that varying the strain at the onset of martensitic hardening does not play a significant role in the strain control of the system. The cases with higher superelastic plateau (cases 3 and 4) provide superior strain control. The peak modified strains in the pgv of 20 cm/s graphs tend to reach a maximum at 0.5 seconds, while for the pgv of 40 cm/s this value tends to be lower, around 0.3 seconds. Owing to the non-linear nature of these systems, the maximum strains seen for the systems having a pgv of 40 cm/s are generally 55-60% higher than those having a pgv of 20 cm/s for cases 1 and 2, and 50-55% higher for cases 3 and 4. In all systems, the strain increase approaches a near-constant value for non-modified periods of 1 second or greater. Response modification of systems having long natural periods results in relatively small increases in strain.

The addition of supplemental damping (dotted lines) resulted in maximum strains lower than their non-modified counterparts. This can be seen for all cases and hysteretic schemes. The strain reductions seen in Figure 6 appear to be the greatest through the period range of 0.2 – 0.8 seconds for all results. In this range, the strains have been reduced by 30-70%, depending on the case and the hysteretic scheme.

Figure 7 shows the mean maximum strain response to the far-field earthquakes. The strain increases as a result of response modification are smaller than those for near-field earthquakes. The differences observed in Figure 7 between 6% and 8% martensite strains are practically negligible, and thus the martensitic hardening strain plays a lesser role in the system behaviour. Once again, a higher superelastic stress plateau contributes to superior strain control (cases 3 and 4).

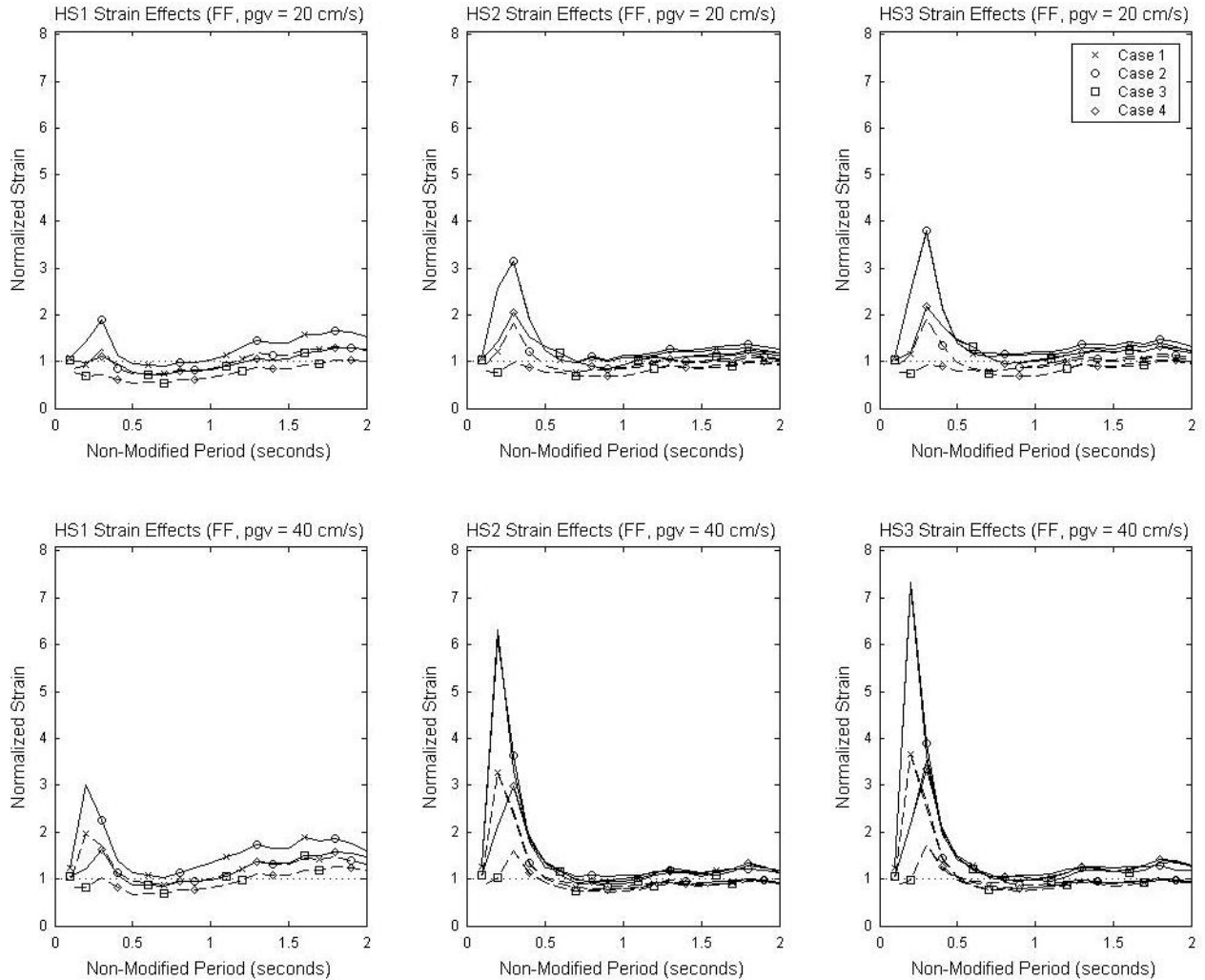


Figure 7. Maximum strain response for far-field earthquakes (solid line – 5% damping, dashed line – 25% damping)

Figure 8 shows the stress in the SMA element for the near-field earthquakes. The normalized maximum stresses shown in the graphs have been determined by taking a ratio of modified stresses to the base non-modified case for that period. Figure 8 shows that the stresses in the SMA element have been reduced in many of the hysteretic schemes and earthquake scalings. The results show a trend of *increasing* stress with less energy dissipation capacity (HS1 → HS3), and with earthquakes with greater peak ground

velocities. In the case of HS3 for a pgv of 40 cm/s, the stresses have increased by close to 40% (compared to their non-modified counterparts) in the 0.3 second region, which is in direct opposition to the aim of seismic isolation. This type of behaviour can also be observed in Figure 4. The results are better for cases with high superelastic plateau stresses. The introduction of supplemental damping creates a significant improvement in this situation, with stresses decreasing by more than 50% for HS3 (40 cm/s pgv) in the period range from 0.2 – 2 seconds. This indicates that in designing SMA response modification devices for expected severe ground motions, the usefulness of SMA materials may be more in their self-centring capabilities than in providing substantial damping. Supplemental damping may have to provide control of stresses.

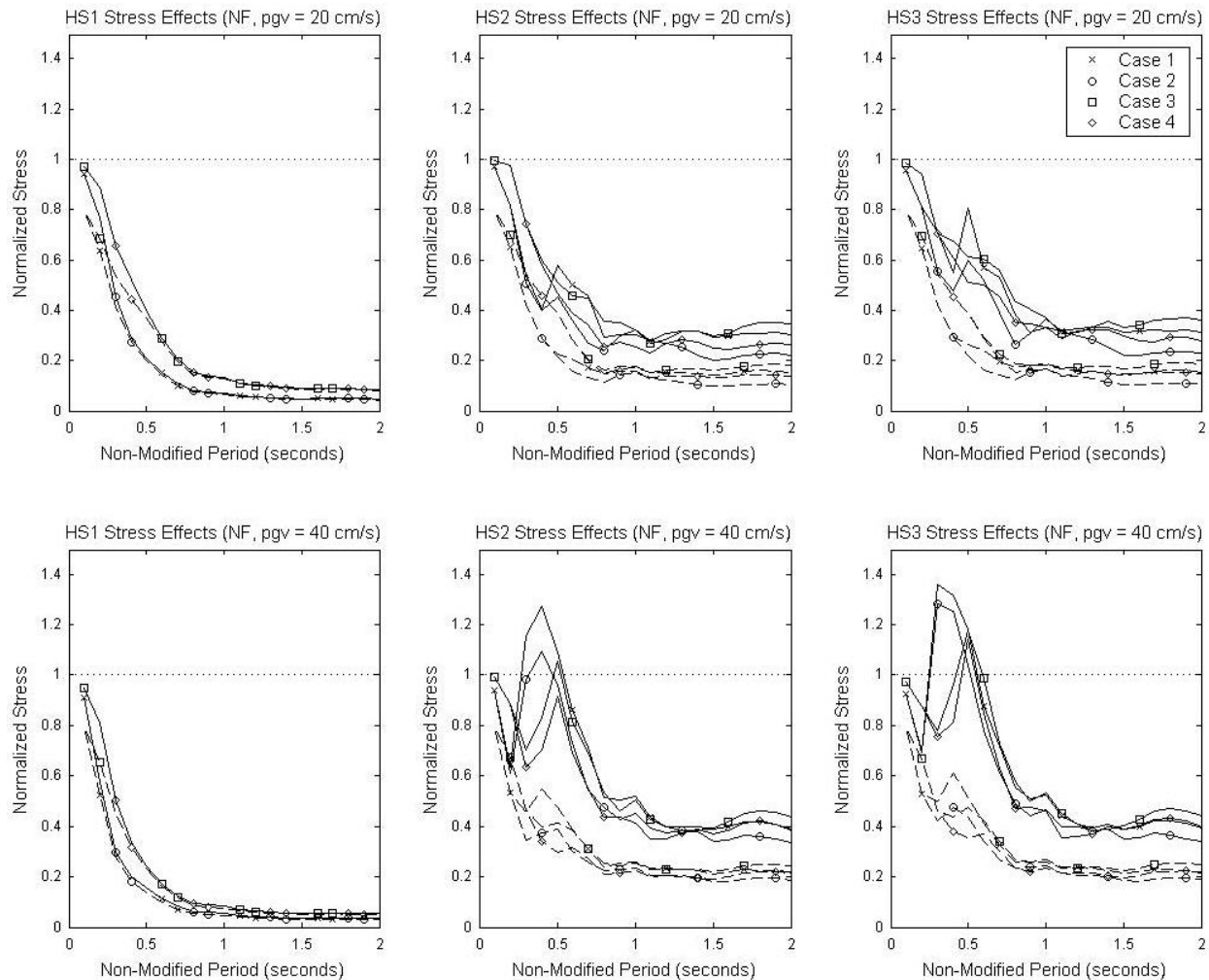


Figure 8. Maximum stress response for near-field earthquakes (solid line – 5% damping, dashed line – 25% damping)

For the far-field earthquakes, unlike the near-field responses, the modified stresses shown in Figure 9 are exclusively less than their non-modified counterparts. This is a direct reflection of the shape of the response spectra for both sets of earthquakes (not shown), where the near-field motions have significant spectral peaks at longer periods. The modified cases (1 and 2) with lower superelastic stress plateaux generally provide greater stress reduction, with the exception of the cases having a lower martensitic strain (cases 1 and 3) value subjected to the 40 cm/s pgv ground motions. This is due to the earlier onset of

martensitic hardening, which causes the stresses to increase at a lower strain for the more severe ground motions (HS1 has no martensitic hardening).

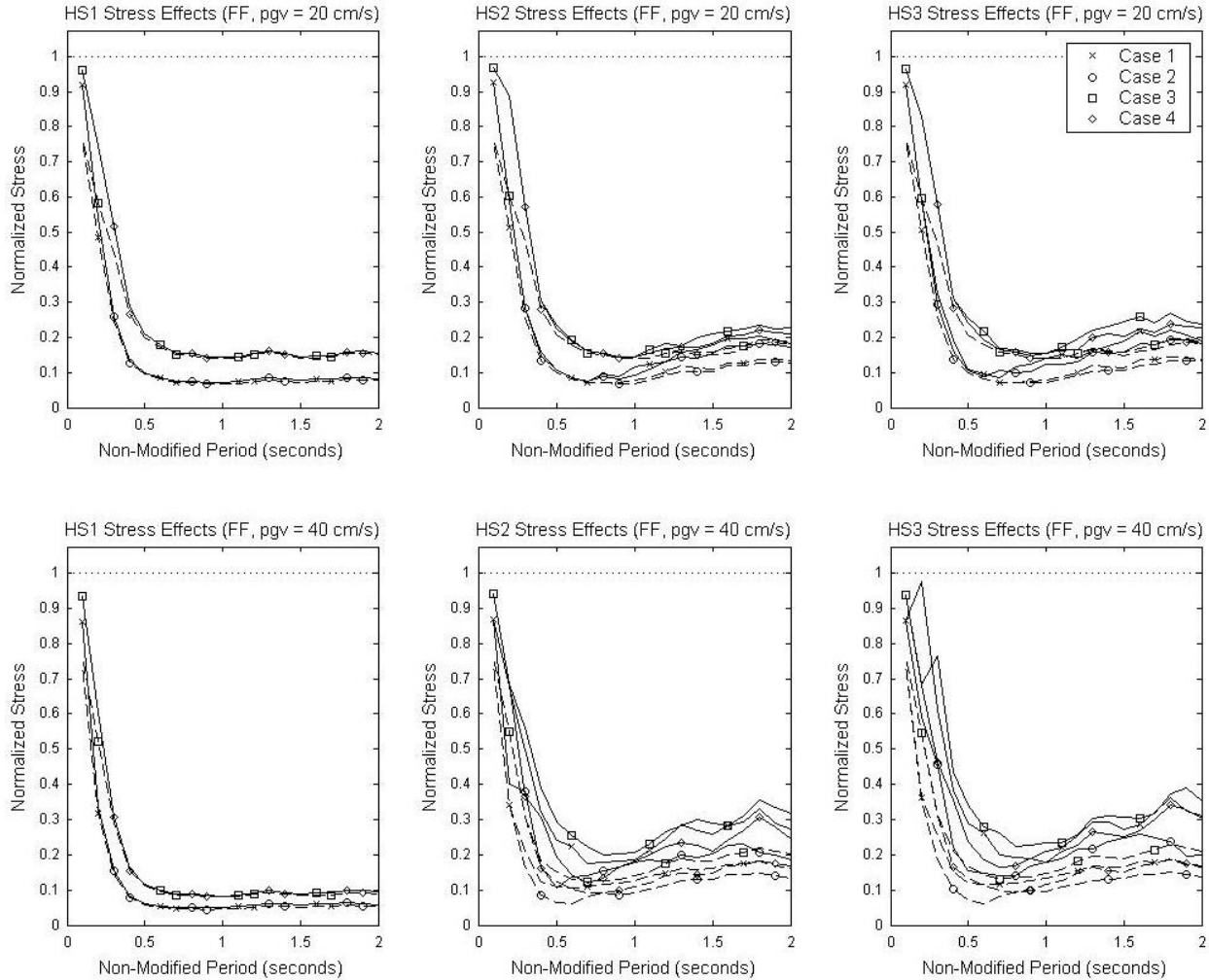


Figure 9. Maximum stress response for far-field earthquakes (solid line – 5% damping, dashed line – 25% damping)

Unity Period

The normalized maximum strain ratios for the near-field earthquakes, shown in Figure 10, have been determined by taking a ratio of maximum strain recorded during the time-history to the strain (ϵ_m) at the completion of transformation to martensitic hardening. The martensitic hardening phase of SMA behaviour is generally used as a safeguard against excessive strains. Operating the SMA devices past their martensitic hardening strain can lead to diminished energy dissipation capacity. Further, at strains approaching 15% or more, SMAs can begin to act plastically, which negates their self-centring capabilities. Thus, it is desirable to limit the strain of SMAs to levels below their martensitic hardening range. In this context it is useful to define a ‘unity period’ as the non-modified period at which the maximum strain ratio line crosses the unity line (and thus the SMA acts in its martensitic range). As such, Figure 10 is useful in determining at which non-modified period a hysteretic scheme will no longer provide adequate structural control. Since this study was performed using stresses and strains, this ‘unity period’ can be shifted by altering the physical characteristics (e.g. length, cross-sectional area) of the specific SMA device in question in order to change the stiffness of the system.

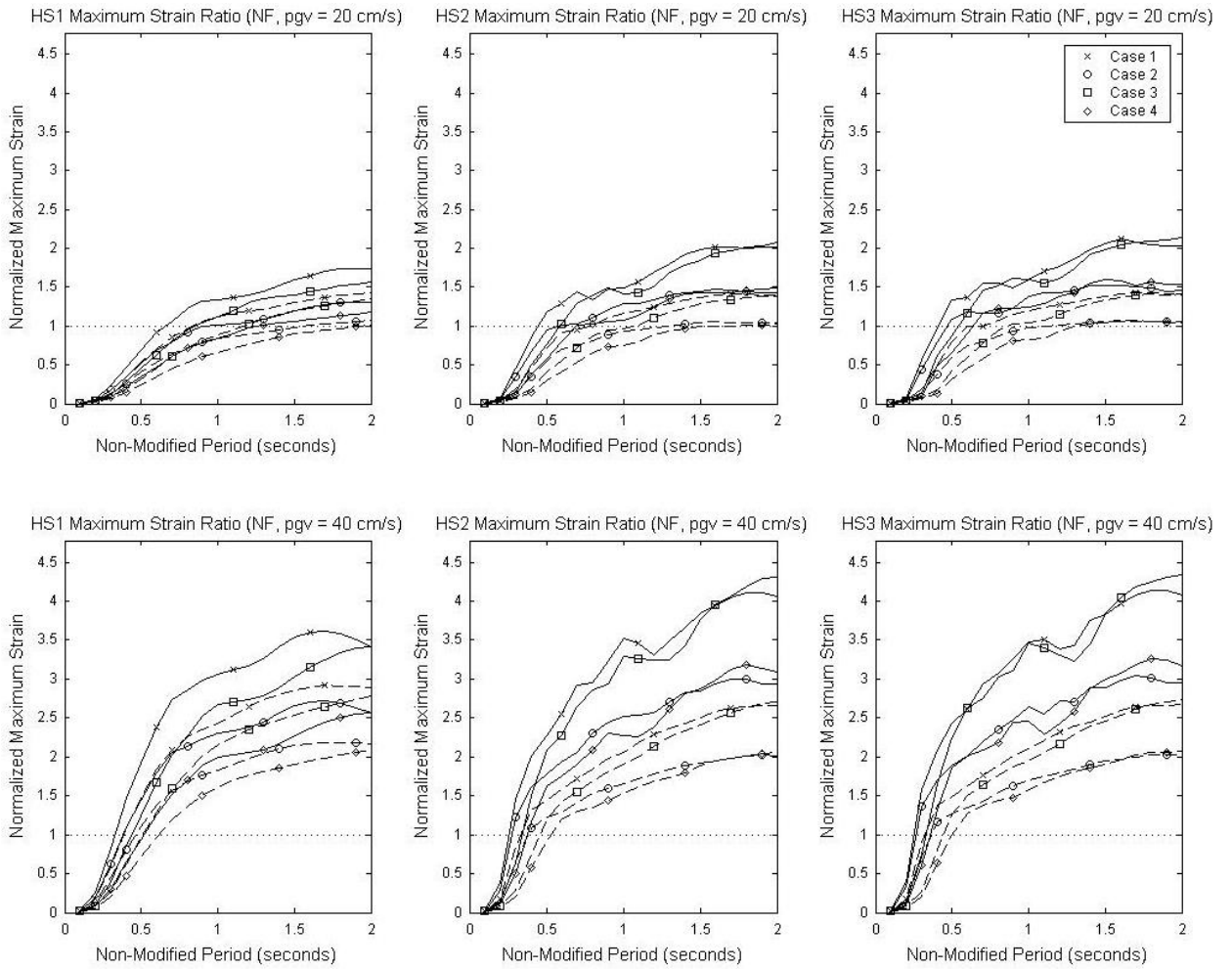


Figure 10. Maximum strain ratios for near-field earthquakes (solid line – 5% damping, dashed line – 25% damping)

From Figure 10 it can be seen that for lower intensity ground motions (20 cm/s), HS1, HS2 and HS3 at 5% damping all reach plateau levels after a non-modified period of about 1.5 seconds. This plateau is generally above the unity line, meaning that the system may approach or exceed strain levels that will cause plastic deformation in the martensite. The cases which have a martensitic hardening strain of $\epsilon_m = 6\%$ naturally provide the greatest exceedences of strain past their martensitic hardening value. The results for the ground motions having a pgv of 40 cm/s have considerably larger strains than for the lower intensity cases. The addition of supplemental damping significantly improves the response for all cases and hysteretic scenarios. For a non-modified period of 2 seconds, HS3 cases 1 and 3 have strains that exceed 400% of the martensitic hardening strain, which implies a strain of 24%. This strain is obviously far past the point of plastic yielding of martensite, and in greatest likelihood, the material would fracture. This leads to the conclusion that the response modification system as defined by this scenario is insufficient under these loading conditions. As mentioned previously, one possible solution to this problem would be to alter the physical dimensions of the SMA material in question to increase the stiffness of the system (thus providing more strain control), or to increase the supplemental damping. The former solution would have the drawback of increasing the system acceleration and velocity.

The far-field strain ratios seen in Figure 11 are noticeably lower than for those seen in Figure 10. The lower intensity earthquakes (20 cm/s) provide strains that are almost entirely lower than their martensitic hardening strains. The results seen for the higher intensity earthquake (40 cm/s) are an improvement over their near-field counterparts, but they still peak at a value over 2 times greater than the strain at martensitic hardening. This shows that SMA response modification systems for far-field earthquakes require less relative stiffness compared to those for near-field earthquakes, in order to avoid the system's operation in the martensitic region.

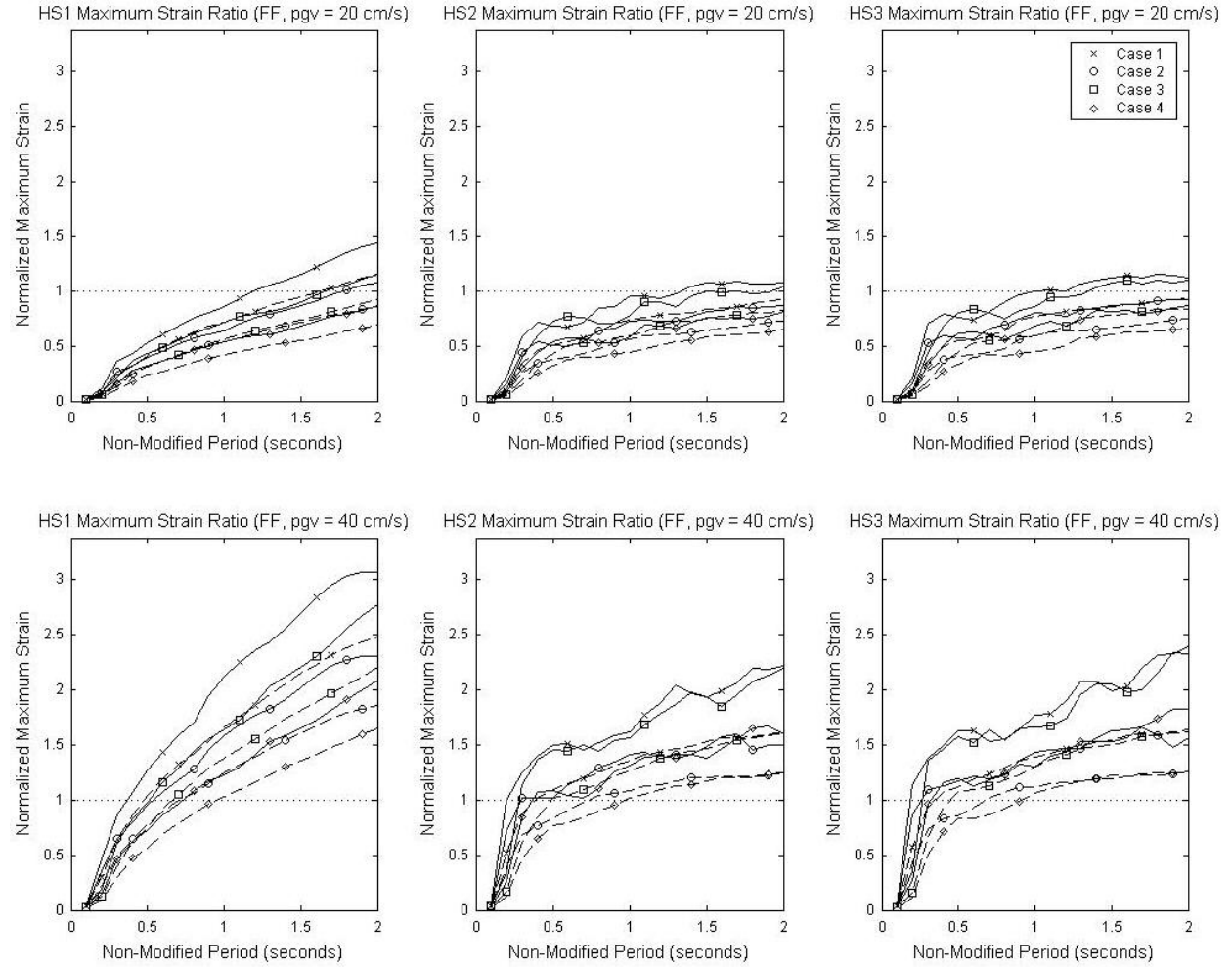


Figure 11. Maximum strain ratios for far-field earthquakes (solid line – 5% damping, dashed line – 25% damping)

CONCLUSIONS

The following conclusions may be drawn from this work:

1. Varying the martensitic hardening strain (ϵ_m) does not play a significant role in the strain or stress control of the system. However, increasing the superelastic plateau of the hysteretic behaviour provides significantly superior strain control but produces little differences in stress control.
2. Increases in strain as a result of response modification for near-field earthquakes are larger than those for far-field earthquakes. Near-field earthquakes also produced higher stress responses. This

- highlights the need for caution when designing response modification systems where near-field events are expected.
3. Systems having lead-rubber type isolation behaviour generally incurred lower strains and stresses than SMA-based systems. A disadvantage of lead-rubber systems however, is the residual strains that require recentring. SMA-based systems provide for automatic recentring.
 4. Modification (with lead-rubber or SMA elements) of elastic systems having a period in the range of 0.2 – 0.7 seconds resulted in stresses that exceeded their non-modified counterparts when subjected to large near-field earthquake motions. These increases in stresses may be effectively controlled with the addition of supplemental damping. In this situation, the usefulness of SMA materials may be limited to their self-centring capabilities.
 5. There exists a ‘unity period’ above which modification of the physical characteristics (e.g. length, cross-sectional area) of the SMA element are necessary to avoid the system responding into its (large strain) martensitic range. This ‘unity period’ varies with hysteretic parameters and ground motion scaling, and is considerably longer for far-field than for near-field ground motions. The addition of supplemental damping also increases the ‘unity period’.

REFERENCES

1. Funakubo H. “Shape memory alloys.” New York: Gordon and Breach Science Publishers, 1987.
2. Clark PW, Aiken ID, Kelly JM, Higashino M, Krumme RC. “Experimental and analytical studies of shape memory alloy dampers for structural control.” Proceedings of SPIE – The International Society for Optical Engineering, Smart Structures and Materials: Passive Damping, San Diego, CA, March 1-2, 1995, 2445: 241-251.
3. Dolce M, Cardone D, Marnetto R. “Implementation and testing of passive control devices based on shape memory alloys.” Earthquake Engineering and Structural Dynamics 2000; 29(7): 945-968.
4. Chopra AK, Chintanapakdee C. “Comparing response of SDF systems to near-fault and far-fault earthquake motions in the context of spectral regions.” Earthquake Engineering and Structural Dynamics 2001; 30(12): 1769-1789.
5. Kelly JM. “The role of damping in seismic isolation.” Earthquake Engineering and Structural Dynamics 1999; 28(1): 3-20.
6. Graesser EJ, Cozzarelli FA. “Shape-memory alloys as new materials for aseismic isolation.” Journal of Engineering Mechanics 1991; 117(11): 2590-2608.
7. Wilde K, Gardoni P, Fujino Y. “Base isolation system with shape memory alloy device for elevated highway bridges.” Engineering Structures 2000; 22(3) 222-229.
8. Clough RW, Penzien J. “Dynamics of Structures.” New York: McGraw Hill, 1993.